Influence of Extrusion Temperature on Molecular Architecture and Crystallization Behavior of Peroxide-Induced Slightly Crosslinked Poly(L-lactide) by Reactive Extrusion

Masumi Takamura,[1,2] Masataka Sugimoto,[2] Seigou Kawaguchi,[2] Tatsuhiro Takahashi,[2] Kiyohito Koyama[2]

[1]*Functional Chemicals & Polymers Research Laboratory, NOF Corporation, 82, Nishimon, Taketoyo-cho, Chita-gun, Aichi 470-2345, Japan*
[2]*Graduate School of Science and Engineering, Yamagata University, 4-3-16 Jonan, Yonezawa 992-8510, Japan*

Received 4 December 2010; accepted 4 April 2011
DOI 10.1002/app.34618
Published online 16 August 2011 in Wiley Online Library (wileyonlinelibrary.com).

ABSTRACT: The influence of temperature during reactive extrusion of poly(L-lactide) (PLLA) on the molecular architecture and crystallization behavior was investigated for *OO*-(*t*-butyl) *O*-(2-ethylhexyl) peroxycarbonate-modified polymer. The long chain–branched PLLA (LCB-PLLA) content and its structure in the resulting slightly crosslinked PLLA (χ-PLLA) containing linear and LCB-PLLA were characterized by both analyses, size exclusion chromatography equipped with multiangle laser light scattering and rheological measurements. A reduction of LCB-PLLA content in χ-PLLA and an increase of number of branches in LCB-PLLA were found with increasing the extrusion temperature. An increase of extrusion temperature induces different process in the polymer: decrease of the lifetime of peroxide, increase of the radical concentration due to rapid peroxide decomposition rate, and increase of the chain diffusion to the amorphous phase. Among these indices, the lifetime of peroxide is a good index for crosslinking behavior of PLLA during extrusion. As for the isothermal crystallization behavior from the melt, the Avrami crystallization rate constant of χ-PLLA increases as an increase of LCB-PLLA content in χ-PLLA. This implies that LCB-PLLA acts as a nucleating agent for PLLA. Furthermore, regime analysis and the free energy of nucleus of χ-PLLA were investigated using Hoffman–Lauritzen theory. © 2011 Wiley Periodicals, Inc. J Appl Polym Sci 123: 1468–1478, 2012

Key words: biopolymers; crosslinking, crystallization; reactive extrusion; structure–property relations

INTRODUCTION

Poly(L-lactide) (PLLA) is the most important key plastic of a biodegradable and biobased aliphatic polyester produced by polymerization of the renewable fermentation product lactic acid in a sense of one not derived from petroleum resources. The high mechanical strength and modulus of PLLA enable it to be used as an alternative to commodity plastics such as polystyrene, polyethylene, and polypropylene. However, the poor processability and low crystallization rates for PLLA often limit its applicability. To overcome these disadvantages, numerous studies on improvement of these disadvantages have been reported.

As for the improvement of poor processability, various methods have been used to introduce a branched architecture into the PLLA, including chemical crosslinking,[1,2] radiation-induced crosslinking,[1,3,4] and peroxide-induced crosslinking.[1,2,5–10] To overcome the low crystallization rates, an addition of inorganic or organic nucleating agents such as clay,[11,12] low-molecular weight organic compounds,[13] and different structured polylatctides including long chain–branched PLLA (LCB-PLLA)[8,14,15] and poly(D-lactide) is the most viable method.[16] Although an individual method of improvement for these two disadvantages is required, an introduction of LCB-PLLA can be compatible to improve both. Among the methods for introducing long chain branches in PLLA, the peroxide-induced crosslinking process by the addition of small amount of peroxide to PLLA during extrusion has been widely accepted because of its simplicity.

In a previous article,[10] we reported the details of the relationship between the type of peroxide and peroxide-induced crosslinking of PLLA by a single-screw extruder. In the case of slowly decomposed peroxides, the weight-averaged molecular weight (M_w) of the peroxide-induced slightly crosslinked

Correspondence to: M. Takamura (masumi_takamura@nof.co.jp).

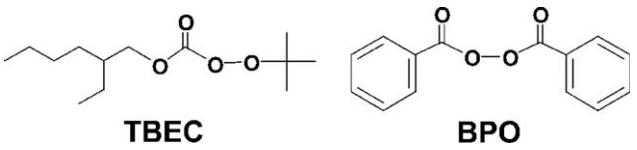

Scheme 1 Chemical formulas and peroxide abbreviations used in this study.

PLLA (χ-PLLA) increased with increasing overall hydrogen abstraction ability of peroxide. On the other hand, in the case of rapid decomposition peroxides such as dibenzoyl peroxide, the M_w and the gel fraction of χ-PLLA were higher than for the slowly decomposed peroxides despite the lower hydrogen abstraction ability.

In a recent article,[15] LCB-PLLA in χ-PLLA induced by various types of slowly decomposition peroxide in a corotating twin-screw extruder was characterized using size exclusion chromatography equipped with multiangle laser light scattering (SEC-MALS), and the results were interpreted according to the hydrogen abstraction ability of peroxide. It is clear that the content of LCB-PLLA with a high M_w increases with increasing the overall hydrogen abstraction ability times the mole ratio of radical number per PLLA precursor molecule. Furthermore, as for the nonisothermal crystallization behavior of χ-PLLA, branch point and entanglement density have remarkable affects on the nucleation rate, the overall crystallization rate and the degree of overall crystallinity.

On the other hand, as for the χ-PLLA induced by rapid decomposition peroxide, its branching structure was not characterized and this seems to be different compared with slowly decomposed peroxide.[10] An increase of the extrusion temperature induces different process in the polymer: decrease of the peroxide lifetime, increase of the concentration per time of radical derived from decomposition of peroxide, and increase of the chain diffusion to the amorphous phase. To clarify the influence of peroxide lifetime on LCB-PLLA architecture and crystallization behavior of χ-PLLA by corotating twin-screw extruder, the extrusion temperature dependence on the above properties of χ-PLLA induced by the medium decomposed peroxide with relatively high-hydrogen abstraction ability (*OO*-(*t*-butyl) *O*-(2-ethylhexyl) peroxycarbonate, TBEC) was investigated.

EXPERIMENTAL

Materials

Commercial grade PLLA (LACEA H100, D-configration; 1.5%, residual lactide; 0.14%) was provided by Mitsui Chemicals (Tokyo, Japan). The melt flow index was 13.1 g 10 min^{-1} (190°C, 2.16 kg). The absolute number-averaged molecular weights (M_n) and weight-averaged (M_w) molecular weights measured by SEC-MALS were 55,100, and 81,500 g/mol, respectively.

Two peroxides were selected as shown in Scheme 1: TBEC and dibenzoyl peroxide (BPO). They were obtained from NOF Corporation (Tokyo, Japan) and were used as received.

Sample preparation

Molecular characterizations of χ-PLLAs sample are shown in Table I. All χ-PLLAs were obtained at

TABLE I
Molecular Characterization of Linear and Slightly Peroxide-Induced Crosslinked PLLA

Sample codes	Lifetime of peroxide[e] (s)	Molar mass[f]		As extruded[g]	
		$M_w \times 10^{-4}$ (g mol^{-1})	M_w/M_n	MFI[h] (g 10 min^{-1})	Gel fraction[i] (wt %)
Neat PLLA	–	8.2	1.48	13.1	–
PLLA[a]-200°C[d]	–	7.8	1.52	13.6	–
PLLA[a]-215°C[d]	–	7.7	1.52	13.6	–
PLLA[a]-230°C[d]	–	7.7	1.53	13.8	–
TBEC[b]-200°C[d]	38	16.0	2.01	3.3	2.0
TBEC[b]-215°C[d]	12	14.8	1.91	3.9	3.1
TBEC[b]-230°C[d]	4	13.5	1.85	5.2	4.4
BPO[c]-200°C[d]	3	13.3	1.89	4.7	5.9

[a] Extruded neat PLLA without peroxide.
[b] TBEC: *OO*-(*t*-butyl) *O*-(2-ethylhexyl) peroxycarbonate. Chemical structure is shown in Scheme1. Radical content was fixed at 2 mol per PLLA molecule (18.15 mmol-peroxide/1 kg PLLA).
[c] BPO: dibenzoyl peroxide. Chemical structure is shown in Scheme1. Radical content was fixed at 2 mol per PLLA molecule (18.15 mmol-peroxide/1kg-PLLA).
[d] Outlet temperature of extruder.
[e] Lifetime at extrusion temperature calculated using decomposition parameter (ΔE and A).
[f] Absolute mean molecular weight measured by SEC-MALS.
[g] Properties of extruded linear or peroxide-induced slightly crosslinked PLLA (χ-PLLA) contained gel.
[h] Melt flow index (190°C × 2.16 kg).
[i] Weight percent of gel after filtration (0.5 μm) of 0.2 wt % χ-PLLA in chroloform.

concentrations of 18.15 mmol-peroxide/1 kg PLLA corresponding to two radical per PLLA precursor (55,100 g mol^{-1}). Crosslinking was carried out by reactive extrusion within a corotating twin-screw extruder PCM-30 (Ikegai, Tokyo, Japan; $D = 30$ mm, $L/D = 30$) with a fixed screw speeds (100 r.p.m) consisting of three thread starts. The extrusion time was around 120 s, measured as the stagnation time of the sample in the extruder from the inlet to the outlet. Previous studies have described the steps of the crosslinking procedure.[10] Three types of extrusion temperature were preset along the extruder from the feeder to the die: (1) 180, 190, 200, and 200°C (at die); (2) 195, 205, 215, and 215 (at die); (3) 210, 220, 230, and 230°C (at die), in the order that the lifetime of peroxide becomes short. The lifetime of peroxide is one of the measures used to quantify the rate of decomposition and defined here as the time when the ratio of residual peroxide to initial peroxide is 0.0001. Therefore, lifetime can be calculated using the thermal decomposition parameters of the peroxides according to the following equation:

$$\text{Lifetime}(s) = -\frac{\ln(0.0001)}{k_d} = -\frac{\ln(0.0001)}{A\exp(-\Delta E/\text{RT})} \quad (1)$$

where k_d (s^{-1}) is the first-order rate constant of each peroxide, both A (s^{-1}) and ΔE (J mol^{-1}) are the decomposition parameters (A: 1.36×10^{15} s^{-1} for TBEC and 4.22×10^{14} s^{-1} for BPO, ΔE: 1.32×10^5 J mol^{-1} for TBEC, and 1.38×10^5 J mol^{-1} for BPO).[17] T is the extrusion temperature at outlet of extruder (200°C = 473 K, 215°C = 488 K, or 230°C= 503 K) and R is the gas constant (8.31 J mol^{-1} K^{-1}). To calculate the lifetime of peroxide, the preset temperature at outlet of extruder is used as T because of the following reason. The molten resin temperature at outlet of extruder is about 10°C higher than the preset temperature. Thus, this leads to 10°C higher than each preset temperature along the extruder from the feeder to the die. For example, type 1 of actual resin temperature is assumed to be 190, 200, 210, and 210°C (at die) while the extrusion preset temperature is 180, 190, 200, and 200°C. Therefore, the mean actual molten resin temperature is same as the preset temperature (200°C) at outlet of extruder. The χ-PLLA samples crosslinked by peroxide at a certain temperature were named "Peroxide abbreviation-extrusion temperature at outlet of extruder" such as "TBEC-200°C." To investigate the molecular architecture and crystallization behavior of χ-PLLA, all χ-PLLA samples were obtained by evaporating the gel-filtrated (<0.5 μm) 0.2 wt % chloroform solution of the extruded χ-PLLA.

As shown in Table I, it is note that all χ-PLLA samples give higher molar mass (M_w and M_w/M_n) and lower MFI compared with corresponding linear PLLA (neat PLLA, PLLA-200°C, PLLA-215°C, and PLLA-230°C, respectively) while the extruded PLLA samples without peroxide are slightly degraded. In this article, PLLA-200°C is defined as corresponding linear PLLA compared with χ-PLLAs.

Second, it is also noted that TBEC-230°C and BPO-200°C samples are χ-PLLAs induced by peroxide with closed short lifetime despite different peroxide type and extrusion temperature.

Furthermore, TBEC-200°C sample in Table I is used the same χ-PLLA sample described as TBEC-2 in a recent article.[15]

Molecular architecture

SEC-MALS

The SEC-MALS eluent was selected as 1,1,1,3,3,3-hexafluoro-2-propanol (HFIP) because of its good solubility and relatively large differential refractive index for polyesters. The eluent contains 10 mM sodium 1,1,1-trifluoroacetate to yield a reasonable chromatogram. The detailed devices and conditions were described in a recent article.[15]

In the branched polymers, the shrinking factor g, which is the ratio of the mean-squared radius of gyration of branched polymer $\langle R_g^2\rangle_b$ to that of linear polymer $\langle R_g^2\rangle_l$ at the same molecular weight, is introduced as defined by the following equation:[18]

$$g = \frac{\left\langle R_g^2 \right\rangle_b}{\left\langle R_g^2 \right\rangle_l} \quad (2)$$

The SEC-MALS technique provides information on another important branching characteristic, the number of branches per molecules m and the LCB frequency λ. The relationship between both m and λ and the g parameter depends on the branching functionality and MWD of the sample. These results suggest that χ-PLLAs are four-armed randomly branched polymers created by the bimolecular recombination of PLLA radicals with an effective radical number per PLLA precursor molecules n that is less than 1.2 as mentioned in a recent article.[15] For the four-armed randomly branched polymer that does not contain any cyclic or networked polymers, the shrinking factor g_4 may be expressed in terms of the number of branches per molecule m of a monodisperse sample at the narrow fraction eluted by the SEC column, as follows[18]:

$$g_4 = \left[\left(1 + \frac{m}{6}\right)^{\frac{1}{2}} + \frac{4m}{3\pi}\right]^{-\frac{1}{2}} \quad (3)$$

The λ can be calculated, defined as the number of branches per repeat unit for PLLA ($R = 72$ g mol^{-1}), as follows:

$$\lambda = \frac{Rm}{M} = 72\frac{m}{M} \quad (4)$$

Rheological measurements

The branching character such as the complex architecture for linear and branched polymer cannot be detected directly by SEC-MALS, rheological measurements in shear flow and elongation can provide a hint in addition.

Shear viscoelastic measurements were determined using ARES (TA Instruments, Tokyo, Japan) under a nitrogen atmosphere at 180°C. The detailed procedure was described in a recent article.[15] To represent the angular frequency dependence of the dynamic complex viscosity $|\eta^*|$ for the linear PLLA (PLLA-200°C), or the χ-PLLA, the generalized Cross-Carreau-Yasuda model[19] was used, and the zero shear viscosity η_0 was obtained according to the following equation:

$$|\eta^*| = \eta_0[1 + (\lambda_m\omega)^a]^{(l-1)/a} \quad (5)$$

where λ_m, a, and l are model constants.

Uniaxial elongational viscosity at constant strain rates (0.05–1.0 s^{-1}) was measured using ARES (TA Instruments) with elongational mode under nitrogen atmosphere at 180°C. The test specimens (10 mm width, 30 mm length, and 0.6 mm thickness) were cut from a sheet at the same manner as shear viscoelastic measurements.

Crystallization behavior

Isothermal crystallization characterization was performed using differential scanning calorimeter (DSC-7, Perkin Elmer, CA) under a nitrogen flow (10 mL min^{-1}) in a temperature range from 100 to 150°C. Before DSC, the samples were dried in a vacuum oven for 1 week at 70°C, and the DSC samples (about 5 mg, 100-μm-thick) were cut from a sheet that had been prepared by compression molding at rapid 200°C min^{-1} cooling from the melt (220°C in 10 min). Initially, the sample was heated at 10°C min^{-1} from 25 to 220°C and held for 5 min at 220°C to erase the thermal history. After this process, the rapid cooling to the crystallization temperature at −200°C min^{-1} was estimated to observe the kinetics of isothermal crystallization. To describe the isothermal crystallization, the Avrami equation[20,21] below is widely used:

$$X(t) = 1 - \exp[-K(t - t_i)^n] \quad (6)$$

where $X(t)$ is the relative crystallinity with time calculated by the integration of the isothermal crystallization DSC exotherms for the linear PLLA or the χ-PLLA, K is the Avrami crystallization rate constant, n is the Avrami exponent, and t_i is the initial crystallization time defined as the time, which is beyond 0.1% relative crystallinity, respectively. To calculate K and n, the double logarithm of eq. (6) provides a linear relationship,

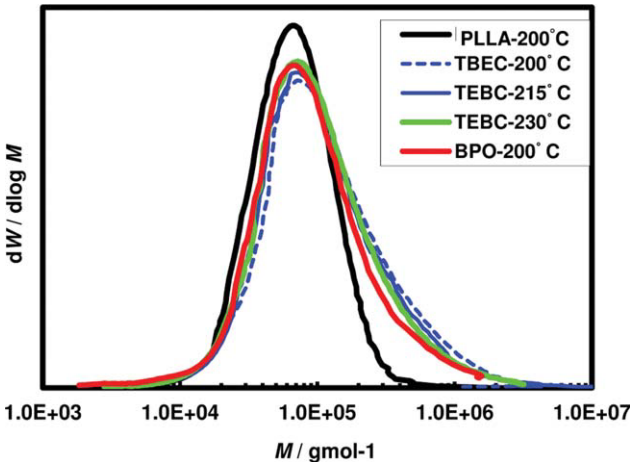

Figure 1 Molecular weight distribution of linear and peroxide-induced crosslinked PLLA obtained by *OO*-(*t*-butyl) *O*-(2-ethylhexyl) peroxycarbonate (TBEC) and dibenzoyl peroxide (BPO). The temperature after the hyphen indicates the extrusion temperature. [Color figure can be viewed in the online issue, which is available at wileyonlinelibrary.com.]

$$\log[-\ln[1 - X(t)]] = \log K + n\log(t - t_i) \quad (7)$$

Accordingly, K and n can be obtained from the slope and intercept, respectively, in a plot of log $[-\ln [1 - X(t)]]$ versus log $(t - t_i)$. For the isothermal crystallization to minimize the possible errors associated with data manipulation, Muller et al.[22] proposed that a linear portion of about 5–20% relative crystallinity was used to obtain K and n. The crystallization half time $(t - t_i)_{1/2}$ can be calculated from K, as shown in the following expression:

$$(t - t_i)_{1/2} = \left(\frac{\ln 2}{K}\right)^{1/n} \quad (8)$$

The crystallization morphology was observed using polarized optical microscope (BX40, Olympus Corporation, Tokyo, Japan) with a hot stage and temperature controller (LK3001, Linkam, UK). Isothermal crystallizations were carried out at 140°C and the size of spherulites formed after 30 min were compared each other.

RESULTS

Molecular architecture of χ-PLLA

Molecular characterization estimated by SEC-MALS

Figure 1 presents molecular weight distribution (MWD) curves for the linear PLLA (PLLA-200°C) and χ-PLLAs induced by TBEC with different

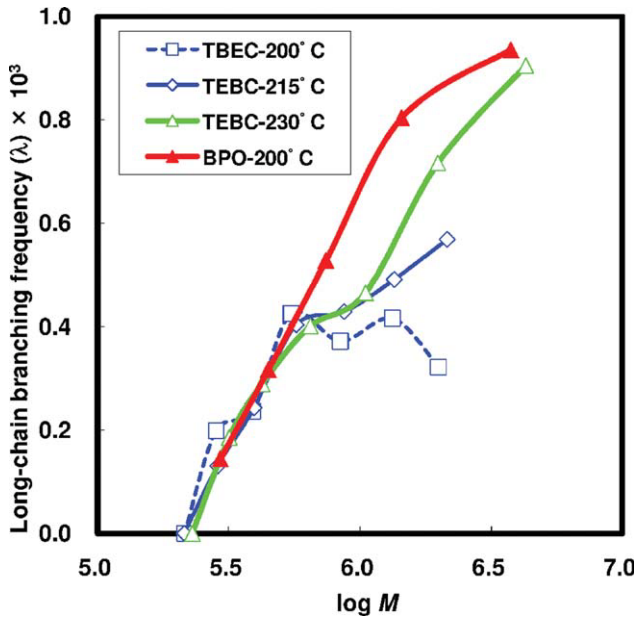

Figure 2 Long-chain branching frequency λ as a function of weight-averaged molecular weight M_w for peroxide-induced slightly crosslinked PLLA obtained by *OO*-(*t*-butyl) *O*-(2-ethylhexyl) peroxycarbonate (TBEC) and dibenzoyl peroxide (BPO). The temperature after the hyphen indicates the extrusion temperature. [Color figure can be viewed in the online issue, which is available at wileyonlinelibrary.com.]

extrusion temperature. Parent linear PLLA (PLLA-200°C) shows a monomodal MWD. In remarkable contrast, the MWD of χ-PLLA clearly shows a tail in the higher molecular weight region as decreasing with the extrusion temperature.

Figure 2 shows the number of branches per repeat unit for PLLA (λ) calculated from eq. (4) as a function of molecular weight for χ-PLLA. Because the highest M_w of linear PLLA (PLLA-200°C) is around $10^{5.7}$ g mol^{-1} as shown in Figure 1, it is assumed that each fraction more than $10^{5.7}$ g mol^{-1} in the SEC chromatogram is considered to be the content only from the branched species while each fraction of χ-PLLAs less than $10^{5.7}$ g mol^{-1} is considered to be the mixture of coeluted linear and branched species. Applying this assumption, λ for LCB-PLLA increases with increasing extrusion temperature so that the average λ-value more than $10^{5.7}$ g mol^{-1} for TBEC-200°C, TBEC-215°C, and TBEC-230°C is 0.38 $\times$ 10^{-3}, 0.46 $\times$ 10^{-3}, and 0.61 $\times$ 10^{-3} per L-lactic acid unit, respectively.

On the other hand, the two χ-PLLAs (TBEC-230°C and BPO-200°C) with closed short lifetime show similar MWD (see Fig. 1), M_w (see Table I) and λ curve (see Fig. 2) regardless of the peroxide type and extrusion temperature.

Molecular characterization estimated by rheological measurements

Figure 3 shows the double-logarithmic plot of the zero shear viscosity η_0 versus the M_w measured by SEC-MALS for linear PLLA (PLLA-200°C) and χ-PLLAs. In addition, the values for several linear PLLA are included, which were measured in a previous investigation,[6] and it was found that the experimentally determined values for several linear PLLA are very well described by the relation $\log \eta_0 = -14.6 + 3.7 \log M_w$ by the full line. As can been seen from Figure 3, the η_0 for linear PLLA (PLLA-200°C) lies slightly below the line representing the relationship of several linear PLLAs (by the full line in Fig. 3) which is, however, within the accuracy of the measurements. The relationship between the η_0 and the M_w can be used for the detection of LCB-PLLA as it was shown in several investigations that the MWD has no effect on this relationship,[23] whereas it is well known from literature that the power law found for linear polymers does not hold for polymers with LCB-PP. Thus, the deviations of the η_0 for χ-PLLAs from the relationship found for linear PLLAs (by the full line in Fig. 3) can be attributed to the influence of the LCB-PLLA.

On the other hand, Figure 4 shows the uniaxial elongational viscosity $\eta_E^+(t, \varepsilon)$ of χ-PLLAs at various Hencky strain rates ε and 180°C comparing with the linear PLLA (PLLA-200°C). All χ-PLLAs show a strain hardening behavior increasing with strain rate while the linear PLLA (PLLA-200°C) coincides with linear viscoelastic regime at all strain rates.

Gabriel and Munstedt[24] investigated the correlations between the type of strain hardening of LCB-polyethylenes (LCB-PE) and the level of their η_0 in comparison with linear PE. For PE of various branching structures four different types of strain

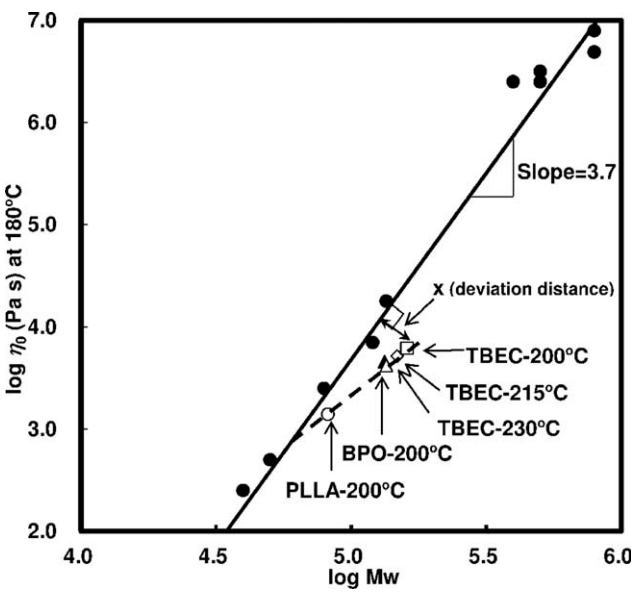

Figure 3 Zero shear viscosity η_0 as a function of weight-averaged molecular weight M_w for peroxide-induced slightly crosslinked PLLA obtained by *OO*-(*t*-butyl) *O*-(2-ethylhexyl) peroxycarbonate (TBEC) and dibenzoyl peroxide (BPO).

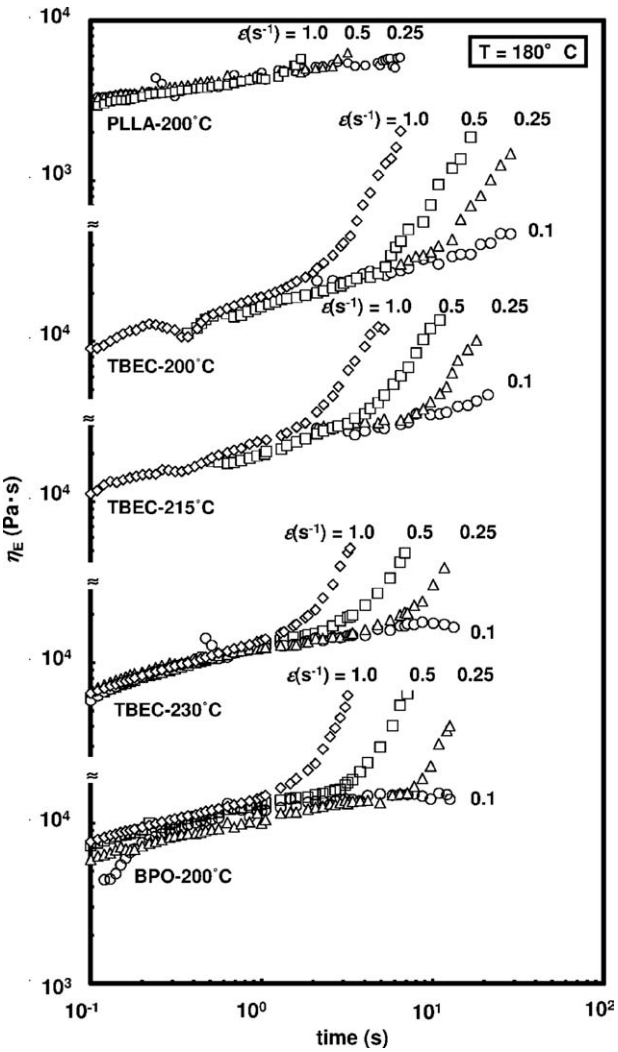

Figure 4 Elongational viscosity $\eta_E^+(t, \dot{\varepsilon})$ as a function of time t at different Hencky strain rates $\dot{\varepsilon}$ for peroxide-induced slightly crosslinked PLLA obtained by *OO*-(*t*-butyl) *O*-(2-ethylhexyl) peroxycarbonate (TBEC) and dibenzoyl peroxide (BPO).

hardening can be observed. Type I, metallocene-catalyzed LCB-linear low density PE (LCB-mLLDPE): strain hardening is approximately independent of elongational rate. Type II, high density PE (HDPE): strain hardening decreases with increasing elongational rate. Type III, LDPE: strain hardening increase with increasing elongational rate. Type IV, mLLDPE: strain hardening is not shown. On the other hand qualitative correlations with the dependence of η_0 on M_w can heuristically be deducted. PE of type IV fulfills the well-established η_0 on $M_w^{3.4}$, samples of types I and II give higher η_0 than the linear PEs. Type III samples generally exhibit η_0 lower than the linear relationship. From Figures 3 and 4, all χ-PLLAs belong to type III, and these show tree-like architecture same as LDPE.

Munstedt et al.[25] reported that the high content of polypropylene with LCB in the blends of a linear and a LCB fall into strain hardening prominent and large deviation from the M_w–η_0 relationship of linear polypropylene. Applying this relationship, it was found that for the reactive extrusion at elevated temperature induced by TBEC the strain hardening is more prominent and the deviation from the M_w–η_0 relationship of linear PLLA defined as deviation distance x in Figure 3 increase. This implies that an increase of LCB-PLLA content as well as x took place with increasing the extrusion temperature.

As for BPO-200°C and TBEC-230°C, both two same plots in Figure 3 and two similar uniaxial elongational flows in Figure 4 show similar molecular architectures.

Taken together molecular architecture combined with SEC-MALS and rheological measurements, a reduction of LCB-PLLA content in χ-PLLA and an increase of number of branches in LCB-PLLA were found with increasing the extrusion temperature.

Isothermal crystallization behavior

Isothermal crystallization characterization of linear PLLA (PLLA-200°C) and χ-PLLAs was performed using DSC in a temperature range from 100 to 150°C. The data of the Avrami exponent n, the isothermal crystallization rate constant K, and the crystallization halftime $(t\text{-}t_i)_{1/2}$ are listed in Table II. Each curve exhibits a good linear relationship, suggesting that the isothermal crystallization kinetics were in good agreement with the Avrami equation, that is, the correlation coefficient r^2 is closed to one. The n-values are close to 2 for linear PLLA (PLLA-200°C) and 3 for all χ-PLLAs (TBEC-200°C, TBEC-215°C, TBEC-230°C, and BPO-200°C), respectively. This suggested that crystallization mode for linear PLLA (PLLA-200°C) and all χ-PLLAs was of two- and three-dimensional growth, respectively, with heterogeneous nucleation.[26] The n-values for linear PLLA (PLLA-200°C; $n = 2$) were smaller than those reported for pure PLLA (= 3 at crystallization temperature T_c = 90–130°C by Kolstad et al.[27] and Iannace and Nicolais et al.[28]). The value difference attributes to the differences in the method for monitoring crystallinity and in the relative crystallinity range used for calculation. The K-values in Table II are plotted in Figure 5 as a function of T_c. As shown in Figure 5, T_c at K maximum for linear PLLA (PLLA-200°C) is around 110°C, and this is similar to that reported by many researchers.[29–32]

On the other hand, first, T_c at K maximum for TBEC-230°C has two maximums (first, around 130°C and second, around 110°C). The second maximum curve for TBEC-230°C is the same for linear PLLA, and the first maximum curve is higher than the second. This curve with two maximum peaks is similar to that for linear PLLA reported by some

TABLE II
Crystallization Parameter of Linear PLLA and Peroxide-Induced Slightly Crosslinked PLLA

Sample codes[a]	T_C[b] (°C)	t_i[c] (min)	$(t - t_i)_{1/2}$[d] (min)	n[e]	K[f] (min^{-1})	r^2[g]
PLLA-200°C	100	1.04	8.91	1.72	0.0160	0.9996
	110	0.37	2.23	2.29	0.1103	1.0000
	115	0.78	2.55	2.01	0.1053	1.0000
	120	0.34	3.42	1.93	0.0646	0.9998
	125	0.97	6.58	1.84	0.0216	0.9999
TBEC-200°C	100	1.09	2.60	2.48	0.0648	0.9995
	110	0.83	1.59	2.55	0.2108	0.9995
	120	0.57	1.08	2.59	0.5631	0.9996
	130	0.69	1.06	2.61	0.5825	0.9999
	140	0.98	1.92	2.76	0.1148	0.9998
	150	2.95	4.36	2.90	0.0098	0.9995
TBEC-215°C	100	1.12	2.73	2.39	0.0629	0.9999
	110	0.82	1.63	2.55	0.1996	0.9997
	120	0.67	1.69	2.36	0.1989	0.9999
	130	0.76	1.24	2.55	0.4016	0.9999
	140	1.09	2.54	2.45	0.0705	0.9998
	150	3.24	6.11	2.76	0.0097	0.9996
TBEC-230°C	100	1.23	3.55	2.52	0.0284	0.9999
	110	0.83	2.24	2.14	0.1222	0.9998
	120	0.79	2.81	2.07	0.0819	0.9997
	130	0.80	1.57	2.25	0.2517	0.9998
	140	1.32	2.76	2.27	0.0692	0.9998
	150	4.11	5.44	2.62	0.0082	0.9997
BPO-200°C	100	1.05	3.66	2.64	0.0225	0.9999
	110	0.77	2.19	2.47	0.0999	0.9999
	120	0.76	2.32	2.09	0.0884	0.9996
	130	0.79	1.53	2.30	0.2591	0.9998
	140	1.01	2.36	2.96	0.0550	0.9999
	150	4.03	5.14	2.66	0.0088	0.9997

[a] See Table 1 for sample codes.
[b] Crystallization temperature.
[c] Initial crystallization time defined as the time which is beyond 0.1% relative crystallinity.
[d] Half time of crystallization.
[e] Avrami exponent.
[f] Avrami crystallization rate constant.
[g] Correlation coefficient of Avrami exponent.

researchers.[33–35] Second, T_c at K maximum for TBEC-215°C has also two maximums (first, around 130°C and second, around 110°C), and the first maximum K-value is higher than for TBEC-230°C while maintaining the second maximum curve. Finally, two T_c at K maximum for TBEC-200°C was overlapped and change into one curve (125°C). As for the K-value at maximum for χ-PLLAs induced by TBEC, all χ-PLLAs is higher than for linear PLLA (PLLA-200°C) and increases with decreasing of the extrusion temperature. These results are mentioned at discussion section.

DISCUSSION

Effect of lifetime of peroxide on molecular architecture of χ-PLLA

An increase of the extrusion temperature induces different process in the polymer: decrease of the lifetime of peroxide, increase of the radical concentration due to rapid peroxide decomposition rate, and increase of the chain diffusion to the amorphous phase. Especially, lifetime of peroxide seems to be the most important index, because the crosslinking reaction state is different depending on peroxide lifetime during reactive extrusion (short peroxide lifetime: reaction in solid PLLA, long peroxide lifetime: reaction in molten PLLA).[10]

To investigate the relationship between the lifetime of peroxide and the molecular properties for χ-PLLA, Figure 6 shows the double-logarithmic plot of the lifetime of peroxide versus the M_w measured by SEC-MALS and relative deviation distance D (= x/maximum x) described in Figure 3. The first major result drawn from Figure 6 is that M_w and its polydispersity (M_w/M_n) for χ-PLLA found to decrease linearly with decreasing the lifetime of peroxide. The second major result is that the D defined as LCB-PLLA content decreases linearly with decreasing the lifetime. From these two results,

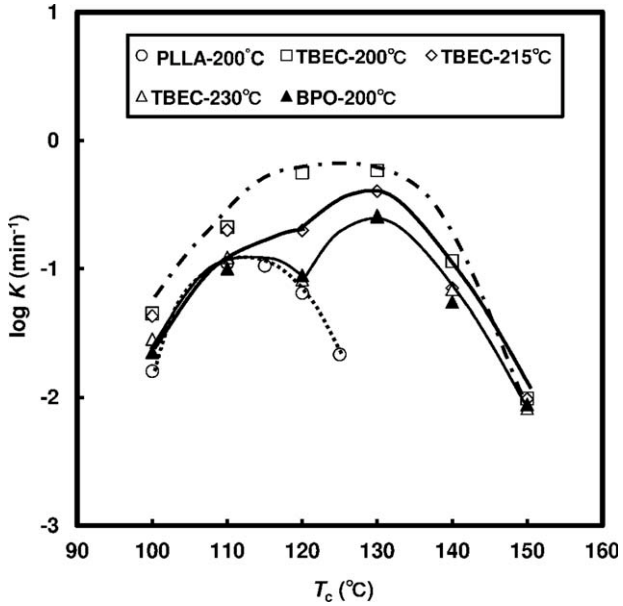

Figure 5 Avrami crystallization rate constants K as a function of crystallization temperature T_c for linear and peroxide-induced slightly crosslinked PLLA obtained by *OO*-(*t*-butyl) *O*-(2-ethylhexyl) peroxycarbonate (TBEC) and dibenzoyl peroxide (BPO).

higher M_w and its polydispersity seem to be caused by higher LCB-PLLA content. Taken together these results with the result of lower degree of branches in LCB-PLLA as a decrease of lifetime, an assumption that peroxide decomposition localized in solid PLLA caused partial crosslinking because of rapid peroxide decomposition can be proved as mentioned in a previous article.[10]

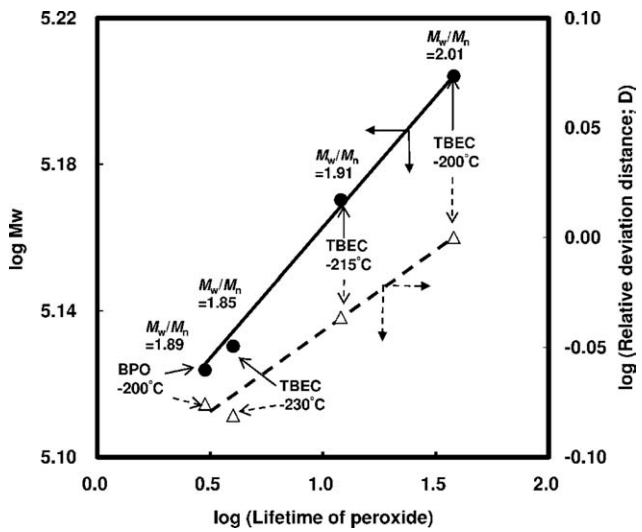

Figure 6 Influence of the lifetime of peroxide on the weight-averaged molecular weight M_w and relative deviation distance D (= x/maximum x) described in Figure 3 for peroxide-induced slightly crosslinked PLLA obtained by *OO*-(*t*-butyl) *O*-(2-ethylhexyl) peroxycarbonate (TBEC) and dibenzoyl peroxide (BPO).

Effect of LCB-PLLA content in χ-PLLA on crystallization behavior

To investigate the relationship between the LCB-PLLA content depending on the lifetime of peroxide and the crystallization behavior, Figure 7 shows the double-logarithmic plot of the D defined as LCB-PLLA content versus the Avrami crystallization rate constant K at 120°C. Figure 7 indicates that K at 120°C suddenly rise when the LCB-PLLA content excess a critical point (D is around $10^{-0.1}$). This result seems to conclude that LCB-PLLA works as a nucleating agent for PLLA like the blends of polypropylene (PP) of LCB-PP.[36]

Using the theoretical approach, it can be shown that the linear growth rate G can be considered proportion to $1/(t - t_i)_{1/2}$ and based on the Hoffman-Lauritzen theory,[37,38] the temperature variation of $1/(t - t_i)_{1/2}$ can be written as:

$$\left(\frac{1}{(t-t_i)_{1/2}}\right) = \left(\frac{1}{(t-t_i)_{1/2}}\right)_0 \exp\left[-\frac{U^*}{R(T_c-T_\infty)}\right] \times \exp\left[-\frac{K_g}{T_c\Delta T f}\right] \quad (9)$$

where K_g is the nucleation constant, ΔT is the degree of under-cooling defined by $T_m^0 - T_c$; T_m^0 is the equilibrium melting point, f is a factor given as $2\ T_c/(T_m^0 + T_c)$, U^* is the activation energy for segment diffusion to the site of crystallization, R is the gas constant, T_∞ is the hypothetical temperature where all motions associated with viscos flow cease ($T_g = 30$ K),

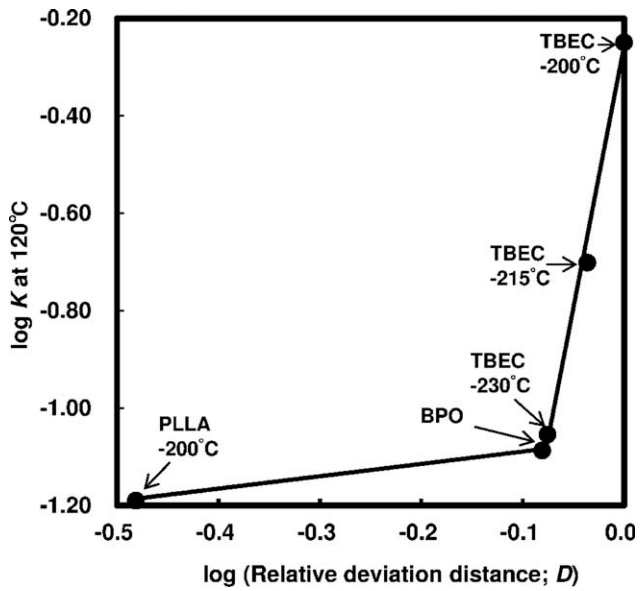

Figure 7 Influence of the relative deviation distance D (= x/maximum x) described in Figure 3 on the Avrami crystallization rate constants K at 120°C for linear and peroxide-induced slightly crosslinked PLLA obtained by *OO*-(*t*-butyl) *O*-(2-ethylhexyl) peroxycarbonate (TBEC) and dibenzoyl peroxide (BPO).

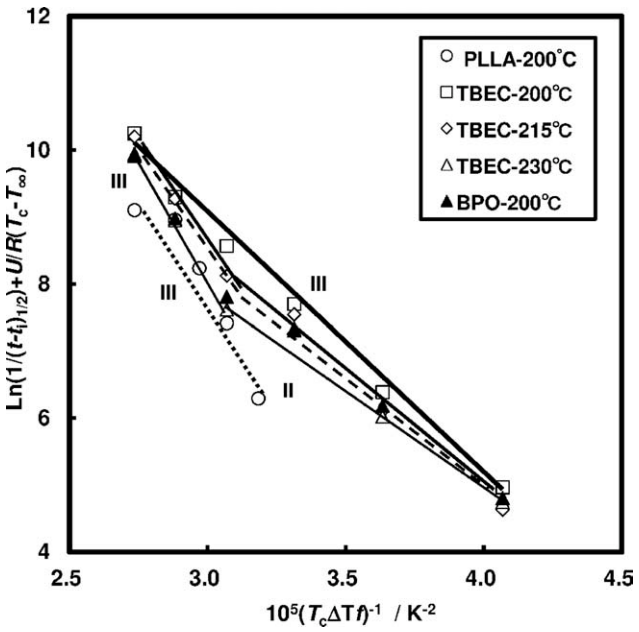

Figure 8 Hoffman-Lauritzen analysis for linear PLLA (PLLA-200°C) and peroxide-induced slightly crosslinked PLLA obtained by *OO*-(*t*-butyl) *O*-(2-ethylhexyl) peroxycarbonate (TBEC) and dibenzoyl peroxide (BPO).

and $[1/(t - t_i)_{1/2}]_0$ is the front factor. For the χ-PLLA that has similar T_m and T_g to linear PLLA reported in previous literature,[39] linear PLLA literature values of $T_m^0 = 215$°C and $T_g = 62.5$°C were used[40] for the calculations. To fit experimental data, $U^* = 1500$ cal/mol was utilized, as done in previous studies on PLLA.[28]

The results of the kinetic data treatment are illustrated in Figure 8. The plot gives K_g as a slope and the intercept ln $[1/(t - t_i)_{1/2}]_0$. From the K_g value obtained by a slope in Figure 8, the surface free energy $\sigma\sigma_e$ can be deduced from the following expression:

$$K_g = \frac{n_a b_0 \sigma \sigma_e T_m^0}{\Delta H_m^0 k} \quad (10)$$

where n_a is a variable that depends on crystallization regime and is equal to 4 for regime I (high temperature) and III (low temperature) and values 2 in regime II (intermediate temperature), b_0 is the thickness of the stem added on the substrate (5.17×10^{-10} m),[41] σ is the lateral surface free energy, σ_e is the free energy of folding, ΔH_m^0 is the enthalpy of fusion (1.11×10^8 J m^{-3}),[42] and k is the Boltzman constant (1.38×10^{-23} J m^{-1}). These calculated values are listed in Table III.

Figure 8 shows that the two different trends were obtained for the linear PLLA (PLLA-200°C) and two χ-PLLAs: (1) linear PLLA (PLLA-200°C) with T_c range of 100–125°C and TBEC-200°C with that of 100–150°C exhibit data fitting well to a single line; (2) TBEC-215°C, TBEC-230°C, and BPO-200°C with T_c range of 100–150°C on the other hand yields two lines with different slopes. As for linear PLLA, the K_g-value (= 6.5×10^5 K^2) and the $\sigma\sigma_e$-value (= 1.0×10^{-3} J^2 K^{-4}) are good agreement with those for linear PLLA in the previous literature ($K_g = 7.6 \times 10^5$ K^2 and $\sigma\sigma_e = 1.2 \times 10^{-3}$ J^{2}K^{-4}; $M_w = 7.5 \times 10^4$ g mol^{-1}),[43] and this slope corresponds to regime III. On the other hand as for TBEC-200°C, the K_g-value (= 4.4×10^5 K^2) and the $\sigma\sigma_e$-value (= 0.68×10^{-3} J^2 K^{-4}) corresponding to regime III are rather lower than those for linear PLLA (PLLA-200°C), and these results seem to lead high *K*. As for TBEC-215°C, TBEC-230°C, and BPO-200°C, the ratio of the two K_g values (TBEC-215°C: 6.0×10^5 and 3.0×10^5 K^2, TBEC-230°C: 6.2×10^5 and 3.1×10^5 K^2 and BPO-200°C: 6.3×10^5 and 3.1×10^5 K^2, respectively) is equal to 2, that is, the same as the value predicted by Lauritzen–Hoffman theory. The transition from regime III to regime II for TBEC-215°C, TBEC-230°C, and BPO-200°C are estimated to occur at 120°C.

As for χ-PLLAs induced by TBEC, the $\sigma\sigma_e$ value for regime III is found to decrease with increasing LCB-PLLA content as well as decreasing extrusion temperature. Combining with the fact that the $\sigma\sigma_e$

TABLE III
Kinetics Results of Linear and Peroxide-Induced Slightly Crosslinked PLLA Using Lauritzen-Hoffmann Equation

Sample codes[a]	Molar mass[b]		K_g[c] $\times 10^{-5}$ (K^2)	$\sigma\sigma_e$[d] $\times 10^4$ (J^2 K^{-4})	Regime	Slope (III/II)
	$M_w \times 10^{-4}$ (g mol^{-1})	M_w/M_n				
PLLA-200°C	7.8	1.52	6.47	9.98	III	–
TBEC-200°C	16.0	2.01	4.38	6.76	III	–
TBEC-215°C	14.8	1.91	5.96	9.21	III	1.97
			3.02	9.61	II	
TBEC-230°C	13.5	1.85	6.21	9.59	III	2.00
			3.11	9.61	II	
BPO-200°C	13.3	1.89	6.29	9.70	III	2.03
			3.09	9.55	II	

[a] See Table 1 for sample codes.
[b] Absolute mean molecular weight measured by SEC-MALS.
[c] Nucleation constant.
[d] Surface free energy of heterogeneous nucleation.

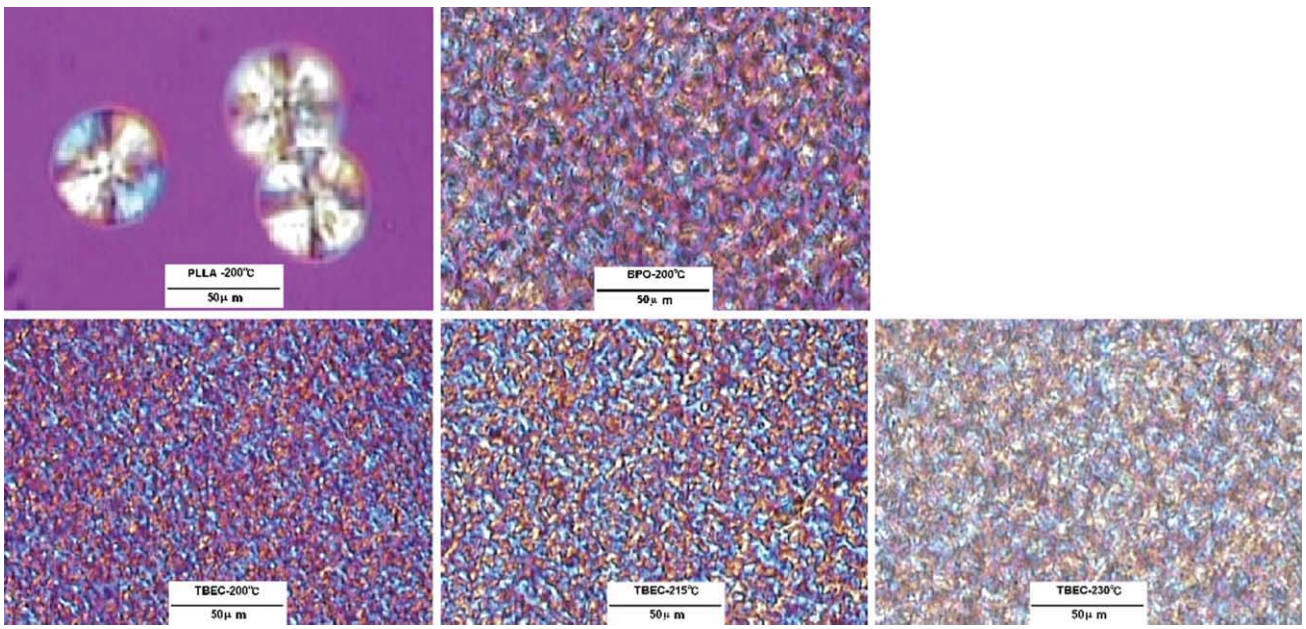

Figure 9 Polarized optical micrographs of the linear PLLA (PLLA-200°C) and peroxide-induced crosslinked PLLA obtained by *OO*-(*t*-butyl) *O*-(2-ethylhexyl) peroxycarbonate (TBEC) and dibenzoyl peroxide (BPO) taken after 30 min of isothermal crystallization at 140°C. [Color figure can be viewed in the online issue, which is available at wileyonlinelibrary.com.]

values of linear PLLA (PLLA-200°C) for regime III is the highest in comparison with χ-PLLAs, this result is the good evidence of LCB-PLLA as a nucleating agent. As for two $\sigma\sigma_e$ values of TBEC-230°C and BPO-200°C with closed peroxide lifetime at each extrusion temperature, they are similar to each other, and it is due to resemble molecular architecture.

Polymer crystallization from the molten state occurs via two main mechanisms: primary nucleation and crystal growth. The crystal growth mechanism on PLLA crystallization has been widely investigated. In the case of crystallization from the melt, the nucleating process is more dominant than the crystal growth process. Two nucleation mechanisms widely accepted are homogeneous and heterogeneous nucleation. The former occurs throughout the random fluctuations of macromolecules that result in favorable alignment of the polymer chains. The latter occurs more commonly at the interface of a second phase. Figure 9 shows the crystallization morphology carried out at 140°C after 30 min by using optical microscopy as the same manner of DSC. The mean size of spherulite is about 50 μm for linear PLLA (PLLA-200°C), 10 μm for BPO-200°C, 5 μm for TBEC-200°C, 7 μm for TBEC-215°C, and 10 μm for TBEC-230°C, respectively. Although not shown in the figures, cystallization mechanism between the linear PLLA (PLLA-200°C) and χ-PLLAs are quite different. The small and large amounts of spherulites for χ-PLLAs arise suddenly in an early period and do not grow larger, while those for linear PLLA (PLLA-200°C) grow gradually after the nucleation. From Figure 9, these all spherulites growth modes seem to be heterogeneous nucleation.

On the other hand, in the case of crystallization from the glassy state, the crystal growth process is more dominant than the nucleating process because of secondary crystal growth on the primary nuclei already existed in the glassy state of polymer. Pantani et al.[33] investigated the *K* for an extruded commercial-grade linear PLLA from the two different states: melt and glass. They observed clearly the different two T_c-values at *K* maximum (105°C: from the melt and 120°C: from the glass). These two T_c values are similar to that (110 and 130°C) for TBEC-215°C, TBEC-230°C, and BPO-200°C, in Figure 5. Furthermore, the *K* curve with T_c at *K* maximum (125°C) for TBEC-200°C seems to be merged by the two *K* curves with T_c at *K* maximum (105°C: from the melt and 120°C: from the glass). The fact that the maximum *K* -value in Figure 5 grows high in the following order: TBEC-230°C, TBEC-215°C, TBEC-230°C = BPO-200°C, linear PLLA (PLLA-200°C) seems to come from the lower $\sigma\sigma_e$-values for regime III (TBEC-200°C: 0.68×10^{-3} J^2 K^{-4}, TBEC-215°C: 0.92×10^{-3} J^2 K^{-4}, TBEC-230°C: 0.96×10^{-3} J^2 K^{-4} = BPO-2 : 0.97×10^{-3} J^2 K^{-4}, linear PLLA (PLLA-200°C): 1.0×10^{-3} J^2 K^{-4}) as shown in Table III. These results were reasonable, given the assumption that the primary crystal nuclei were existed in χ-PLLA at the early stage of rapid under cooling from the melt and the amounts of primary crystal nuclei at the early stage increase with increasing LCB-PLLA. Although the reason where the primary crystal nuclei are derived from is not clear, it may come from

the following three possibilities: the branching point of χ-PLLA, the highly entanglement with itself or linear PLLA derived from insufficient melt due to its high equilibrium melting temperature and the phase separation of branched PLLA from χ-PLLA.

CONCLUSIONS

The influence of temperature during reactive extrusion of PLLA on the molecular architecture and crystallization behavior was investigated for TBEC-modified polymer. The LCB-PLLA content and its structure in χ-PLLA containing linear and LCB-PLLA were characterized by SEC-MALS and rheological measurements. With increasing the extrusion temperature, a reduction of LCB-PLLA content in χ-PLLA and an increase of number of branches in LCB-PLLA were found. Furthermore, from a result of molecular characterization estimated by rheological measurements, molecular architecture for LCB-PLLA seems to be a tree-like LDPE, and it is assumed that the composition ratio of PLLA with LCB increases with increasing of peroxide lifetime.

In the case of isothermal crystallization behavior from the melt, the Avrami crystallization rate constant of χ-PLLA increases as an increase LCB-PLLA content in χ-PLLA. This implies that LCB-PLLA acts as a nucleating agent for PLLA combined with Hoffman–Lauritzen analysis.

As for the χ-PLLA with (TBEC-230°C and BPO-200°C) closed peroxide lifetime despite different peroxide type and extrusion temperature, their molecular architecture and crystallization behavior are similar to each other. This result indicates the lifetime of peroxide is a one of the good index for crosslinking behavior of PLLA during extrusion.

Authors express grateful appreciation to associate professor Go Matsuba, Yamagata University, for valuable suggestions and discussions about crystallization behavior. We also thank to Mr. Daiki Izuta for measurement of SEC-MALS and Dr. Hideyuki Uematsu for melt rheology and DSC, respectively.

References

1. Nijenhuis, A. J.; Grijpma, D. W.; Pennings, A. J. Polymer 1996, 37, 2783.
2. Hartmann, M. H. In Biopolymers from Renewable Resources; Kaplan, D. L., Ed.; Springer-Verlag: Berlin, 1998; Chapter 15.
3. Babanalbandi, A.; Hill, D. J. T.; Whittaler, A. K. Polym Degrad Stab 1997, 58, 203.
4. Milicevic, D.; Trifunovic, S.; Galovic, S.; Suljovrujic, E. Rad Phys Chem 2007, 76, 1376.
5. Sodergard, A.; Nasman, J. H. Polym Degrad Stab 1994, 46, 25.
6. Dorgan, J. R.; Lehermeier, H.; Mang, M. J Polym Environ 2000, 8, 1.
7. Lehermeier, H. J.; Dorgan, J. R. Polym Eng Sci 2001, 41, 2172.
8. Cicero, J. A.; Dorgan, J. R.; Garrett, J.; Runt, J.; Lin, J. S. J Appl Polym Sci 2002, 86, 2839.
9. Takagi, J.; Nemoto, T.; Miyazaki, M.; Nishioka, A.; Takimoto, J.; Koyama, K. Seikei-Kakou 2002, 14, 598.
10. Takamura, M.; Nakamura, T.; Takahashi, T.; Koyama, K. Polym Degrad Stab 2008, 93, 1909.
11. Ray, S. S; Yamada, K.; Okamoto, M.; Ogami, A.; Ueda, K. Chem Mater 2003, 15, 1456.
12. Nam, J. Y.; Ray, S. S.; Okamoto, M. Macromolecules 2003, 36, 7126.
13. Nam, J. Y.; Okamoto, M.; Okamoto, H.; Nakano, M.; Usuki, A.; Matsuda, M. Polymer 2006, 47, 1340.
14. Fujio, I.; Kanaya, T. Polym Prepr Japan 2003, 52, 2511.
15. Takamura, M.; Nakamura, T.; Kawaguchi, S.; Takahashi, T.; Koyama, K. Polym J 2010, 42, 600.
16. Tsuji, H.; Takai, H; Saha, S. K. Polymer 2006, 47, 3826.
17. Brandrup, J.; Immergut, E. H. In Polymer Handbook, 4th ed.; Wiley: New York, 1999; Chapter II.
18. Zimm, B. H.; Stockmayer, W. H. J Chem Phys 1949, 17, 1301.
19. Yasuda, K.; Armstrong, R. C.; Cohen, R. E. Rheol Acta 1981, 20, 163.
20. Avrami, M. J Chem Phys 1939, 7, 1103.
21. Avrami, M. J Chem Phys 1940, 8, 212.
22. Lorenzo, A. T.; Arnal, M. L.; Albuerne, J.; Muller, A. J. Polymer Test 2007, 26, 222.
23. Masuda, T.; Kitagawa, K.; Inoue, T.; Onogi, S. Macromolecules 1970, 3, 116.
24. Gabriel, C.; Munstedt, H. J Rheol 2003, 47, 619.
25. Stange, J.; Uhl, C.; Munstedt, H. J Rheol 2005, 49, 1059.
26. Banks, W.; Sharples, A. Macromol Chem 1963, 59, 233.
27. Kolstad, J. J. J Appl Polym Sci 1996, 62, 1079.
28. Ianace, S.; Nicolais, L. J Appl Polym Sci 1997, 64, 911.
29. Nam, J. Y.; Okamoto, M.; Okamoto, H.; Nakano, M.; Usuki, A.; Matsuda, M. Polymer 2006, 47, 1340.
30. Tsuji, H.; Takai, H.; Saha, S. K. Polymer 2006, 47, 3826.
31. Li, H.; Huneault, M. A. Polymer 2007, 48, 6855.
32. Pantani, R.; De Santis, F.; Sorrentino, A.; De Maio, F.; Titomanlio, G. Polym Degrad Stab 2010, 95, 1148.
33. Di Lorenzo, M. L. Eur Polym J 2005, 41, 569.
34. Yasuniwa, M.; Tsubakihara, S.; Iura, K.; Ono, Y.; Dan, Y.; Takahashi, K. Polymer 2006, 47, 7554.
35. Kawai, T.; Rahman, N.; Matsuba, G.; Nishida, K.; Kanaya, T.; Nakano, M.; Okamoto, H.; Kawada, J.; Usuki, A.; Honma, N.; Nakajima, K.; Matsuda, M. Macromolecules 2007, 40, 9463.
36. Ni, Q. -L.; Fan, J. -Q.; Dong, J. -Y. J Appl Polym Sci 2009, 114, 2180.
37. Hoffman, J. D.; Davis, G. T.; Lauritzen, J. I., Jr. In Treatise on Solid State Chemistry: Crystalline and Non-crystalline Solids; Hannay, J. B., Ed.; Plenum: New York, 1976, 367.
38. Patel, R. M.; Spruiell, J. E. Polym Eng Sci 1991, 31, 730.
39. Yang, S. -I.; Wu, Z. -H.; Yang, W.; Yang, M. -B. Polymer Test 2008, 27, 957.
40. Abe, H.; Kikkawa, Y.; Inoue, Y.; Doi, Y. Biomacromolecules 2001, 2, 1007.
41. Vasanthankumari, R.; Pennings, A. J. Polymer 1983, 24, 175.
42. Hoffman, J. D. Polymer 1983 24, 3.
43. He, Y.; Fan, Z.; Hu, Y.; Wu, T.; Wei, J.; Li, S. Eur Polym J 2007, 43, 4431.